

Magnetic structure in Dy/Sc superlattices

F. Tsui, C. P. Flynn, and R. S. Beach
University of Illinois, Urbana, Illinois 61801

J. A. Borchers, R. W. Erwin, and J. J. Rhyne
National Institute of Standards and Technology, Gaithersburg, Maryland 20899

We have investigated magnetic order in superlattices of Dy and Sc grown along the hcp c axis by molecular beam epitaxy (MBE) techniques. Our neutron diffraction experiments reveal that individual Dy layers order ferromagnetically below $T_c \sim 150$ K. The magnetic coherence length along the growth direction is less than the Dy-layer thickness. Previous studies of rare-earth superlattices with Y or Lu as spacer layers have shown that magnetic coherence propagates through sufficiently thin nonmagnetic interlayers. This arises from the long-range exchange interaction that originates from nesting features in the Fermi surface of the spacer material. The lack of coupling in Dy/Sc superlattices reflects the very different Fermi surface of Sc, with much weaker nesting than Y and Lu.

I. INTRODUCTION

Coherent magnetic properties of rare-earth superlattices have been the subject of great interests since the early 1980s. This is in part the result of advances in materials synthesis using molecular beam epitaxy (MBE), particularly in thin-film growth of rare-earth metals.¹ Studies of single-crystal superlattices of Dy with nonmagnetic Y or Lu as spacer layers have produced a variety of interesting magnetic structures.^{2,3} Two of the most striking results are (1) that the Dy magnetization wave passes through many sufficiently thin intervening spacer layers to form a coherent magnetic structure along the c axis; and (2) that the magnetic phase diagram of Dy epilayers can be drastically altered from that of the bulk material, depending on the sign and strength of lattice strain and the degree of lattice clamping. The observed long magnetic coherence length along the c axis in c -axis Dy/Y and Dy/Lu superlattices is a consequence of the long-range exchange interaction between Dy moments through the conduction electrons, which arises from nesting features in the Fermi surfaces in the superlattices.⁴ The suppressed or enhanced ferromagnetic transition temperatures in the Dy epilayers of the Dy/Y or Dy/Lu systems are driven by magnetoelastic energetics.^{5,6}

In this article we report results from the neutron scattering and superconducting quantum interference device (SQUID) magnetometry measurements on two c -axis Dy/Sc superlattices, c -[Dy₂₅ Å|Sc₄₀ Å]₆₆ and c -[Dy₁₄ Å|Sc₂₁ Å]₈₅ grown by MBE techniques. The 8% lattice mismatch between Dy and Sc presents a unique challenge in epitaxial growth⁷ that is discussed in Sec. II. Sc is yet another nonmagnetic hcp element with a conduction band similar to those of the Y, Lu, and other heavy rare earths. However, these new Dy-based superlattices show very different magnetic behavior from those of the Y or Lu counterparts. The magnetic properties of the Dy/Sc superlattices, such as layer-to-layer magnetic coherence and spin arrangements, are discussed in Sec. III.

II. SAMPLE GROWTH

The Dy/Sc superlattices were grown by MBE techniques following a procedure similar to that used for Dy/Y samples.² Sapphire substrates cut along the $[11\bar{2}0]$ directions were used as the growth templates. A buffer layer of 1000 Å (110) Nb was first grown at a substrate temperature of 900 °C. 1000 Å of (0001) Sc buffer was then deposited at 600 °C. In order to minimize interdiffusion, the superlattice was grown at 350 °C, a temperature 50 °C lower than that used for the Dy/Y superlattices. The deposition rate for the superlattice was reduced to about 0.2 Å/s in an attempt to accommodate the large lattice mismatch and low growth temperature. The conditions above maintained the crystal growth within the "step-flow" regime. The resulting superlattice has a crystal coherence length of about 500 Å along the c axis, a mosaic spread of about 1°, and the effective interdiffusion is limited to several interface layers, as determined by x-ray Bragg scans.

The growing surface was monitored *in situ* by reflection high-energy electron diffraction (RHEED). Figure 1(a) shows a typical RHEED pattern from the surface of a Sc buffer layer. The short, sharp streaks indicate a flat surface with a lateral crystal coherence length > 300 Å. RHEED observation made during the superlattice growth revealed that, for Dy on Sc or vice versa, the first monolayer of the heteroepitaxy was pseudomorphic and then the strain was partially relaxed during the growth of the second monolayer. From the second layer on, the lattice constants in the growth plane stayed constant with a remaining strain of more than 2% for each component. A typical RHEED picture for a Sc surface during the superlattice growth is shown in Fig. 1(b). The broader and longer streaks with respect to that of the buffer layer correspond to a lateral crystal coherence length of about 100 Å.

III. MAGNETIC RESULTS AND DISCUSSION

Neutron scattering experiments on c -[Dy₂₅ Å|Sc₄₀ Å]₆₆ and c -[Dy₁₄ Å|Sc₂₁ Å]₈₅ were carried out on a triple-axis spectrometer at the National Institute of Standards and Technology Reactor. These experiments were designed to probe the spin structure, its coherence, and the tempera-

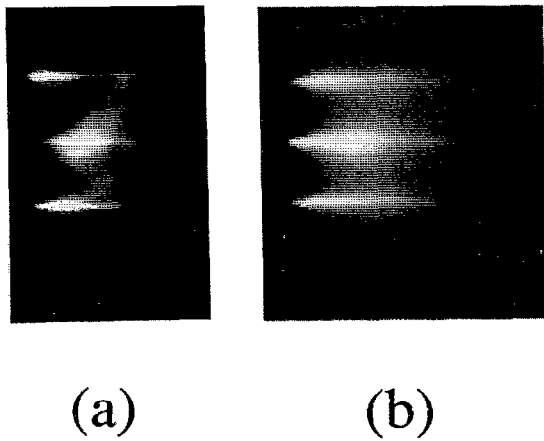


FIG. 1. Typical RHEED pictures for Sc surfaces along the $[11\bar{2}0]$ azimuth: (a) diffraction from a Sc buffer layer surface indicating excellent surface and bulk crystal order, and (b) surface of Sc in a Dy/Sc superlattice. The somewhat longer and broader streaks in (b) reflect a slightly shorter surface coherence.

ture and field dependences. Collimations of $40'-48'-48'$ were used to produce a resolution of 0.03 \AA^{-1} for longitudinal scans. Scans along the c -axis growth direction, namely $(000l)$ scans, were performed near the (0002) Bragg reflection. Figure 2 shows three such scans. In Fig. 2, superlattice sidebands are indicated by arrows, and the (0002) nuclear peak at $Q_{c*}=2.40 \text{ \AA}^{-1}$ of the Sc buffer layer is shown as a reference.

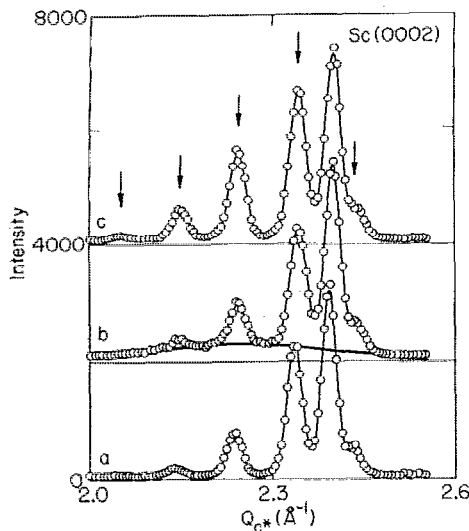


FIG. 2. Neutron diffraction from c - $[\text{Dy}_{25} \text{ \AA} | \text{Sc}_{40} \text{ \AA}]_{66}$ for scans along the $[0002]$ direction: (a) nuclear intensity at 160 K showing five structural superlattice sidebands and (0002) Sc reflection from the buffer layer; (b) zero-field scan at 10 K showing the short-ranged ferromagnetic order along the growth direction that is indicated by the thick line underneath the unchanged structural superlattice peaks; and (c) zero-field-cooled scan at 10 K, at a 60 kOe field applied along the a axis showing the magnetic superlattice intensities on top of structural peaks, indicating a coherent ferromagnetic order with vanishing short-ranged order. Scans (b) and (c) are each displaced by 2000 and 4000 counts for clarity. Lines through the data points are Gaussian fits, and arrows indicate superlattice reflections.

Structural intensity of the superlattice was measured at high temperatures, as shown in Fig. 2(a). The superlattice peak widths coincide with the instrumental resolution. This indicates a structural coherence length $>200 \text{ \AA}$, which is consistent with the x-ray data. At low temperatures additional ferromagnetic intensity was observed as a single broad peak under the superlattice sidebands near $Q_{c*}=2.24 \text{ \AA}^{-1}$, while the intensities of the superlattice peaks remained constant, as illustrated in Fig. 2(b). No basal plane spiral was evident within the temperature range of the experiments. Instead, ferromagnetic transitions occur at $T_c=147 \text{ K}$ for c - $[\text{Dy}_{25} \text{ \AA} | \text{Sc}_{40} \text{ \AA}]_{66}$ and $T_c=100 \text{ K}$ for c - $[\text{Dy}_{14} \text{ \AA} | \text{Sc}_{21} \text{ \AA}]_{85}$, which are much higher than the bulk value of 85 K .⁸ Furthermore, these samples do not order above T_c even through the bulk helimagnetic transition temperature of $\sim 180 \text{ K}$.⁸ For c - $[\text{Dy}_{25} \text{ \AA} | \text{Sc}_{40} \text{ \AA}]_{66}$, the width of the ferromagnetic peak is about 0.35 \AA^{-1} just below T_c , and gradually reduces to about 0.26 \AA^{-1} at 10 K , with an uncertainty of 0.04 \AA^{-1} . The widths correspond to a ferromagnetic coherence length along the c axis of $18 \pm 2 \text{ \AA}$ just below T_c , and $24 \pm 3 \text{ \AA}$ at low temperatures. Thus the ferromagnetic coherence is slightly less than the Dy-layer thickness of 25 \AA below T_c , and extends over each individual Dy layer at low temperatures. Similar behavior is also observed in c - $[\text{Dy}_{14} \text{ \AA} | \text{Sc}_{21} \text{ \AA}]_{85}$. Therefore, spin coupling between neighboring magnetic layers through the Sc interlayers as thin as 21 \AA appears negligible. The observed magnetic intensity at zero field corresponds to isolated thin ferromagnetic Dy layers. The intensity of the ferromagnetic peak, on the other hand, increases with decreasing temperature, which corresponds to the increasing polarization expected for ferromagnetic order.

Field-dependent neutron scattering experiments were also performed. The magnetic field was applied along the a axis in the growth plane to align the spins in the different Dy layers. As the field increases, the intensity of the broad ferromagnetic peak is transferred to the superlattice sidebands. The observed magnetic intensities superposed on the structural superlattice peaks correspond to a coherent ferromagnetic spin structure along the c axis as the Dy moments are aligned by the applied field. Figure 2(c) shows a neutron scan at 10 K with a high field of 60 kOe , in which the coherent ferromagnetic intensities are saturated, while the broad ferromagnetic peak nearly vanishes. The widths of the coherent ferromagnetic peaks coincide, as expected, with the instrumental resolution because the magnetic coherence extends over the entire sample.

Complementary bulk magnetization measurements were performed using a commercial SQUID magnetometer. Figure 3 shows the temperature dependence of the field-cooled and zero-field-cooled magnetizations for c - $[\text{Dy}_{25} \text{ \AA} | \text{Sc}_{40} \text{ \AA}]_{66}$ with fields applied along and perpendicular to the c axis. There is no observable differences between the a - and b -axis magnetizations, so the results for the a - or b -axis fields are presented together as basal plane results. The onset of irreversibility coincides with the development of basal plane ferromagnetic order at $T_c=147$

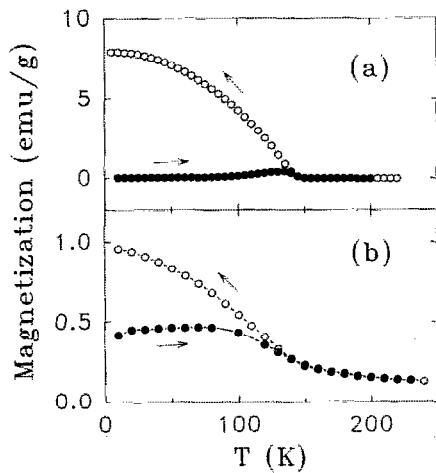


FIG. 3. Temperature dependence of the field-cooled (open circles) and zero-field-cooled (closed circles) magnetizations for c -[Dy₂₅ Å|Sc₄₀ Å]₆₆: (a) 10 Oe field applied perpendicular to the c axis, and (b) 100 Oe field applied along the c axis.

K. The paramagnetic Curie temperatures θ_p determined from magnetization above T_c , along and perpendicular to the c axis are 40 and 140 K, respectively. The disparities in magnetization and in θ_p between the two directions are both consistent with basal plane order. Field-dependent hysteresis loops were also measured for fields applied along various symmetry directions. Figure 4 shows two of such loops at 15 K. The initial basal plane zero-field-cooled field dependences are identical to those obtained from neutron scans with a gradual approach to saturation. At 15 K, the coercive field and remanent magnetization in the basal plane are about 10 kOe and 120 emu/g, respectively. Since the Dy layers are magnetically isolated, the bulk field dependence determines the anisotropy of the individual Dy layers.

The large enhancement of T_c evidently arises from particular structural features of the superlattice, namely from the large strain and strong lattice clamping. It is well established for bulk Dy that the available magnetoelastic en-

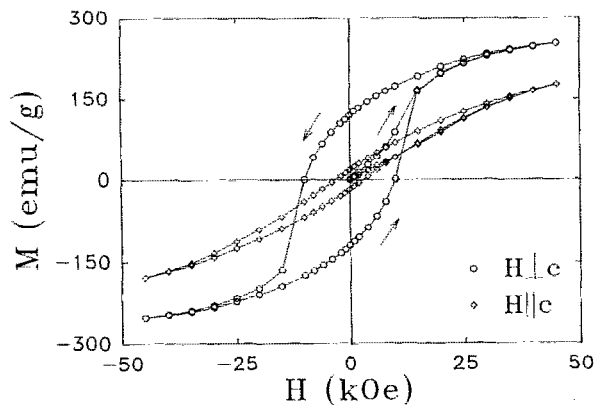


FIG. 4. Hysteresis loops for c -[Dy₂₅ Å|Sc₄₀ Å]₆₆ at 15 K for fields applied perpendicular (circles) and parallel (diamonds) to the c axis.

ergy from the tetragonal distortion, in addition to the crystal field anisotropy, gives rise to a first-order ferromagnetic transition.⁸ In the Dy/Sc superlattice, a tetragonal distortion more than an order of magnitude larger is provided by the Sc and this probably causes the greatly enhanced T_c . The observed large saturation and coercive fields, the strong field-cooled zero-field-cooled irreversibilities, the lack of difference between the a - and b -axis responses, and the small remanent magnetization all point to the presence of an unusually strong and spatially dependent anisotropy field that rigidly "pins" the ferromagnetic domains. These features could be associated with interfacial alloying and dislocations in the superlattices.^{3,5,6}

The lack of interlayer magnetic coherence in the Dy/Sc superlattice reported here suggests that the nesting of the Fermi surface in Sc is much weaker than that in Y or Lu. This is consistent with results from bulk Sc-based alloys.⁹ However, the observed large and randomly distributed anisotropy field, which corresponds to a saturation field of > 50 kOe at 15 K, might overwhelm the much weaker interlayer exchange energy¹⁰ and lock the individual ferromagnetic layers into randomly distributed domains.

In summary, we have studied magnetic order in Dy/Sc superlattices grown along the hcp c axis. Our neutron diffraction and SQUID magnetometry experiments on c -[Dy₂₅ Å|Sc₄₀ Å]₆₆ and c -[Dy₁₄ Å|Sc₂₁ Å]₈₅ reveal that individual Dy layers in the two superlattices order ferromagnetically at $T_c = 147$ and 100 K, respectively. These values are greatly enhanced from the value for bulk Dy of 85 K. No observable magnetic coherence is transmitted through the Sc interlayers as thin as 21 Å. A large isotropic basal plane anisotropy field was observed which may contribute to the negligible interlayer magnetic coherence.

This research is supported in part by NSF Grant No. DMR-88-20888.

¹J. Kwo, D. B. McWhan, E. M. Gyorgy, L. C. Feldman, and J. E. Cunningham, in *Layered Structure, Epitaxy and Interfaces*, edited by J. H. Gibson and L. R. Dawson (MRS, Pittsburgh, 1985), p. 509.

²R. W. Erwin, J. J. Rhyne, M. B. Salamon, J. Borchers, S. Sinha, R. Du, J. E. Cunningham, and C. P. Flynn, *Phys. Rev. B* **35**, 6808 (1987).

³R. S. Beach, J. A. Borchers, A. Matheny, M. B. Salamon, R. W. Erwin, J. J. Rhyne, and C. P. Flynn (unpublished).

⁴Y. Yafet, J. Kwo, M. Hong, C. F. Majkrzak, and T. O'Brien, *J. Appl. Phys.*, **63**, 3453 (1988).

⁵R. W. Erwin, J. J. Rhyne, M. B. Salamon, J. Borchers, R. Du, and C. P. Flynn, *Proceedings of the MRS Neutron Scattering Symposium*, Vol. 166, edited by S. M. Shapiro, S. C. Moss, and J. D. Jorgensen (MRS, Pittsburgh, 1990), p. 133.

⁶F. Tsui, C. P. Flynn, M. B. Salamon, R. W. Erwin, J. A. Borchers, and J. J. Rhyne, *Phys. Rev. B* **43**, 1332 (1991).

⁷The lattice mismatches of Y, Lu, and Sc relative to Dy are 1.7%, -2.5%, and -7.8%, respectively.

⁸J. J. Rhyne, in *Magnetic Properties of Rare Earth Metals*, edited by R. J. Elliott (Plenum, New York, 1972), Chap. 4.

⁹The observed spin-glass behavior in Sc and rare-earth alloys with greater than 75% Sc: H. R. Child and W. C. Koehler, *Phys. Rev.* **174**, 562 (1968).

¹⁰The interlayer exchange in Y-based superlattices resulted in a saturation field of ~ 5 kOe for Y-layer thickness of 40 Å: J. Kwo, in *Thin Film Techniques for Low Dimensional Structures*, edited R. F. C. Farrow, S. S. P. Parkin, P. J. Dobson, J. H. Neave, and A. S. Arrott (Plenum, New York, 1987).